

# Supplemental Materials: Weak dissipation for high fidelity qubit state preparation and measurement

## ESTIMATE OF M1 DECAY RATE

The electronic contribution to the spontaneous M1 decay rate from an excited state  $|n'J'L'S'\rangle$  to a lower energy (by  $\hbar\omega$ ) state  $|nJLS\rangle$  will be given by

$$A_{M1} = \frac{\omega^3}{3\pi\epsilon_0\hbar c^5} \frac{|\langle n'J'L'S' \|\boldsymbol{\mu}\| nJLS \rangle|^2}{(2J'+1)} \quad (S1)$$

where  $\boldsymbol{\mu} = \mu_B(\mathbf{L} + g_s\mathbf{S})$ ,  $g_s$  is the spin  $g$ -factor of the electron (defined to be positive), and  $\mu_B$  is the Bohr magneton. In the limit that these are Russel-Saunders coupled states that are well described by spin and orbital angular momentum quantum numbers  $L$  and  $S$ , we have

$$\begin{aligned} |\langle J'LS \|\boldsymbol{\mu}\| JLS \rangle|^2 &= \mu_B^2 |\langle J'LS \|\mathbf{L}\| JLS \rangle + g_s \langle J'LS \|\mathbf{S}\| JLS \rangle|^2 \\ &= \mu_B^2 (2J+1)(2J'+1) \left| (-)^J \begin{Bmatrix} L & J & S \\ J' & L & 1 \end{Bmatrix} \sqrt{(2L+1)(L+1)L} \right. \\ &\quad \left. + g_s (-)^{J'} \begin{Bmatrix} S & J & L \\ J' & S & 1 \end{Bmatrix} \sqrt{(2S+1)(S+1)S} \right|^2, \end{aligned} \quad (S2)$$

which for a  ${}^2D_{5/2} \rightarrow {}^2D_{3/2}$  fine structure decay is

$$|\langle J'LS \|\boldsymbol{\mu}\| JLS \rangle|^2 = \frac{12}{5} (g_s - 1)^2 \mu_B^2. \quad (S3)$$

For the decay rate of this transition in the  $4f^{14}5d$  fine structure of  $\text{Yb}^+$ , this gives

$$A_{M1} = 2\pi \times 4.5 \text{ mHz} = \frac{1}{36 \text{ s}}. \quad (S4)$$

The  ${}^2D_{5/2} \rightarrow {}^2D_{3/2}$  fine structure decay can also occur via an E2 transition, which is characterized by the rate

$$A_{E2} = \frac{\omega^5}{60\pi\epsilon_0\hbar c^5} \frac{|\langle n'J'L'S' \|\mathbf{Q}\| nJLS \rangle|^2}{(2J'+1)}. \quad (S5)$$

If we estimate that this will occur with an atomic scale electric quadrupole transition moment ( $\langle n'J'L'S' \|\mathbf{Q}\| nJLS \rangle \approx ea_0^2$ ), the E2 contribution to this decay is orders of magnitude smaller than the M1 contribution due to the low frequency.

## DETAILED ENERGY LEVEL DIAGRAM OF ${}^{171}\text{Yb}^+$

Figure S1 shows the energy levels and transitions used in this work. Spontaneous E1 decays from the three highest states branch primarily to the  ${}^2S_{1/2}$  ground state.

## SINGLE QUBIT GATE RANDOMIZED BENCHMARKING

We quantify the fidelity of our single qubit gates by performing randomized benchmarking [1]. Each sequence of length  $l$  consists of  $l$  randomized computational gates, with each computational gate composed of a Pauli gate,  $e^{-i\sigma_P\pi/2}$  such that  $\sigma_P \in \{\pm\sigma_X, \pm\sigma_Y, \pm\sigma_Z, \pm I\}$  followed by a Clifford gate,  $e^{-i\sigma_C\pi/4}$  such that  $\sigma_C \in \{\pm\sigma_X, \pm\sigma_Y\}$ . Pauli identity gates are implemented as delays of length  $t = t_\pi$ , and rotations about the  $z$ -axis are treated as identity gates with a shift in the logical frame for all subsequent gates in the sequence.

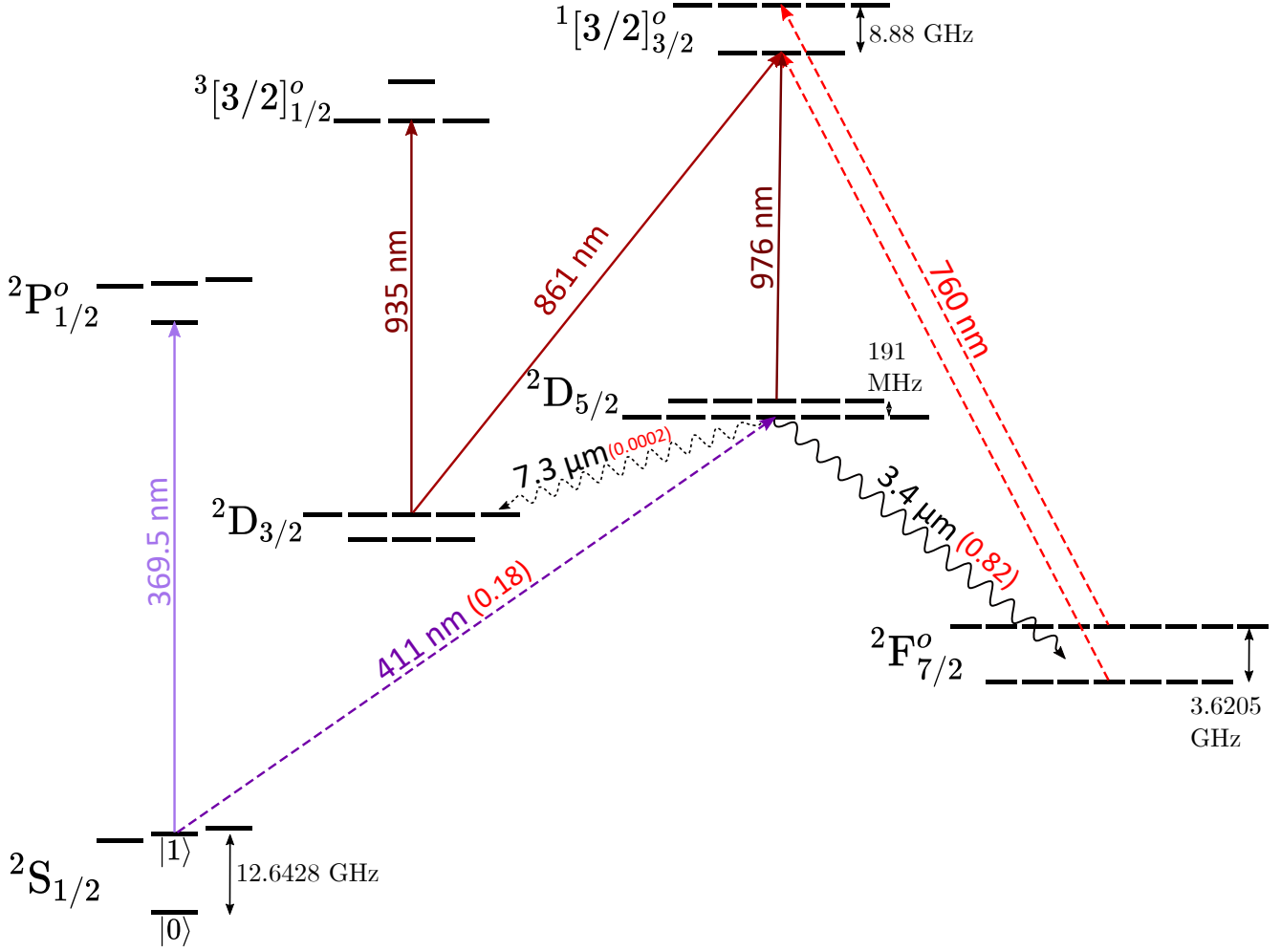


**Figure S1.**  $^{171}\text{Yb}^+$  energy level scheme employed to achieve high fidelity state preparation and measurement of the ground state hyperfine qubit. Electric quadrupole (E2) transitions are shown as dashed, straight lines. The 411 nm E2 transition to the  $^2\text{D}_{5/2}$  is used to shelve population from the  $^2\text{S}_{1/2}(F=1)$  manifold to  $^2\text{F}_{7/2}^o$  via a 3.4  $\mu\text{m}$  decay. The  $^2\text{D}_{5/2}$  states can also decay via a rare M1 transition (dashed, wavy line) to the  $^2\text{D}_{3/2}$  manifold, which we repump using 861 nm light to transfer the population to the  $^1[3/2]_{3/2}^o$  states. Population is out-coupled from the metastable manifold via two 760 nm DBR lasers.

State measurement for the randomized benchmarking experiment is performed by cycling the closed  $^2\text{S}_{1/2}(F=1) \leftrightarrow ^2\text{P}_{1/2}^o(F=0)$  transition. We use sequence lengths  $l \in \{2, 3, 5, 8, 13, 21, 34, 55, 89, 144\}$ , terminating at 144 due to limitations of our pulse sequencer. The benchmarking consists of 1000 unique sequences, with  $N_C = 10$  unique sets of Clifford gates and  $N_P = 10$  unique Pauli randomizations per Clifford set of length  $l$ . The fidelity of each sequence is determined by performing 150 experiments per sequence. During all experiments,  $t_\pi \approx 25 \mu\text{s}$ , corresponding to a Rabi frequency of  $\Omega = 2\pi \times 19 \text{ kHz}$ . All pulses are separated by a delay of 4  $\mu\text{s}$  to allow for proper phase switching of our microwave source.

Randomized benchmarking results are shown in Fig. S2. We measure an average single qubit gate infidelity of  $7.4(1.0) \times 10^{-5}$  for our system, and infer a state preparation and measurement infidelity of  $9.8(6) \times 10^{-3}$  throughout the randomized benchmarking trial, consistent with auxiliary evaluation of our unshelved state preparation and measurement fidelity.

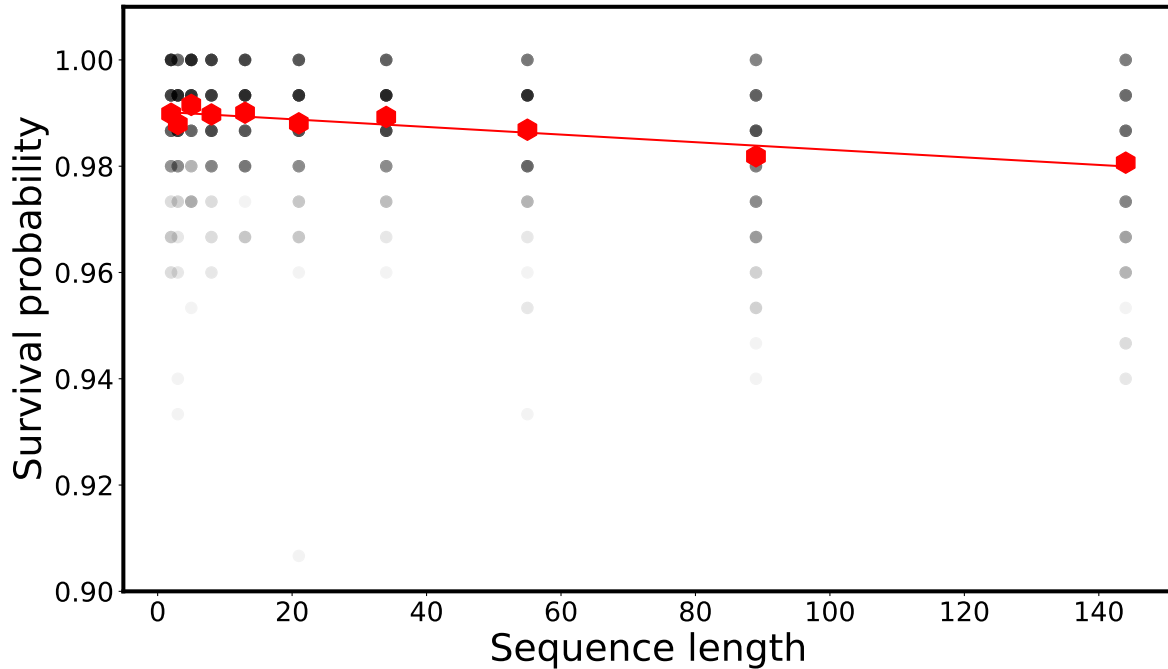


**Figure S2.** Randomized benchmarking to measure the single qubit gate fidelity. The intercept illustrates the unshelved SPAM fidelity and the decay is used to characterize the gate fidelity.

### PRESENTED MEASUREMENTS

From the calibration data set, the state discrimination threshold was chosen such that a successful preparation of the  $|1\rangle$  state would produce an error with probability  $\leq 10^{-7}$  based on the  $|1\rangle$  state distribution mean of the calibration data. The Doppler cooling threshold is similarly chosen such that a properly cooled ion would fail the thresholding with probability  $\leq 10^{-6}$  based on calibration data's Doppler cooling count rate.

The histogram shown in Figure 2 displays the final data set used to assess the SPAM accuracy. When attempting SPAM of the  $|0\rangle$  state, 1 attempt out of 50,000 resulted in identification as  $|1\rangle$  due to being below the discriminator threshold. For the  $|1\rangle$  state, 12 attempts (out of 50,000) resulted in identification as  $|0\rangle$ . These 13 errors give the average SPAM inaccuracy  $\epsilon_{\text{SPAM}} = 1.3_{-0.3}^{+0.4} \times 10^{-4} = -39(1)$  dB, where the quoted uncertainty is the 68% confidence interval calculated using the Wilson method for proportions.

A total of 8 errors in the original data set were identified as being due to ion loss events and removed for the accuracy analysis. Including these as errors yields a total of 21 errors for an infidelity of  $1 - \mathcal{F}_{\text{SPAM}} = 2.1_{-0.4}^{+0.5} \times 10^{-4} = -36.8_{-0.9}^{+1.0}$  dB.

The measurement of how accurately an ion in the  ${}^2S_{1/2}$  manifold can be distinguished from one in the  ${}^2F_{7/2}^o$  manifold yielded 0 inaccuracies out of 557,098 attempts. The 95% confidence upper limit on the inaccuracy is  $< -52$  dB, calculated using the exact interval method of the *NIST/SEMATECH e-Handbook of Statistical Methods*, sec. 7.2.4.1 (<http://www.itl.nist.gov/div898/handbook/>, retrieved August 2021).

---

[1] E. Knill, D. Leibfried, R. Reichle, J. Britton, R. B. Blakestad, J. D. Jost, C. Langer, R. Ozeri, S. Seidelin, and D. J. Wineland, "Randomized benchmarking of quantum gates," *Phys. Rev. A* **77**, 012307 (2008).